WEST-EAST HIGH SPEED FLOW FIELD CONFERENCE
19-22, November 2007
Moscow, Russia

TRANSPARENT BOUNDARY CONDITIONS FOR AEROACOUSTIC PROBLEMS

Ivan L. Sofronov* Nikolai A. Zaitsev* and Olga V. Podgornova*

**Keldysh Institute of applied mathematics, Russian academy of sciences, Miusskaya sq. 4, Moscow*
sofronov@spp.keldysh.ru, zaitsev@spp.keldysh.ru, olgapodgornova@gmail.ru

Key words: transparent boundary conditions, aeroacoustics.

Abstract. Application of transparent boundary conditions (TBCs) obtained by authors for different model problems connected with aeroacoustics is reviewed. Discrete counterparts of these conditions do provide very low and predictable value of the reflections from open boundaries for long simulation time. Despite non-localness in both space and time of TBCs operators, they require reasonable computational costs. We exemplify four different cases of derivation and application of TBCs operators useful for aeroacoustics problems.

1. INTRODUCTION

Development of the nonreflecting artificial boundary conditions on open boundaries of computational domains begins on the middle of last century almost simultaneously with the development of numerical methods for initial boundary value problems. Numerous approaches have been suggested; see reviews[1,2,3,4]. In practice, local boundary conditions in combination with the extension of the computational domain are commonly used due to simplicity, e.g. characteristic-based boundary conditions.

In the paper we discuss so-called *transparent boundary conditions* (TBCs). Such an approach truncates the original unbounded domain and provides the complete identity with the solution in the unbounded domain. The identity is provided due to special pseudodifferential operators on the open boundary, non-local in both space and time.

Let us list known approaches of construction and approximation of TBCs operators having reasonable computational costs:

1. TBCs based on the differential potentials method. Approach has been suggested and is developing by V.S. Ryabenkii and colleagues since 1991, see Ref.[5].
2. TBCs based on the high accuracy approximations of Green functions by Fourier series in space and sums of exponentials in time. This approach has been suggested by I. Sofronov in 1992, Ref.[6], and advanced in Refs.[7,8,9,10].
3. TBCs based on the lacunae property. The possible ways are a) use of Kirchhoff formula[1]; b) algorithms based on difference potentials

mentioned above, see Ref.[11] ; and c) approach of M. Grote and J. Keller Ref.[12,13].

Note that TBCs are not widely used in practice. We think about two possible reasons. Firstly, the coupling of TBCs with a concrete numerical algorithm requires additional and often nontrivial research. Secondly, the perfectly matched layers (PML) approach, also appeared recently[14], becomes very popular due to its simplicity, particularly as to coupling issue.

The main observed drawback of PML is its numerical instability that can appear for long-time calculations. However, aeroacoustics applications require low and predictable value of the reflections from open boundaries for long simulation time. From this point of view TBCs are a good choice.

In the paper we consider our techniques of TBCs constructions, and demonstrate several examples for aeroacoustics problems.

2. TRANSPARENT BOUNDARY CONDITIONS

Numerical simulation of the wave propagation on an unbounded domain requires nonreflecting boundary conditions reducing the infinite physical region to a finite computational domain. Schematically we represent the 2D geometry example as shown in Figure .

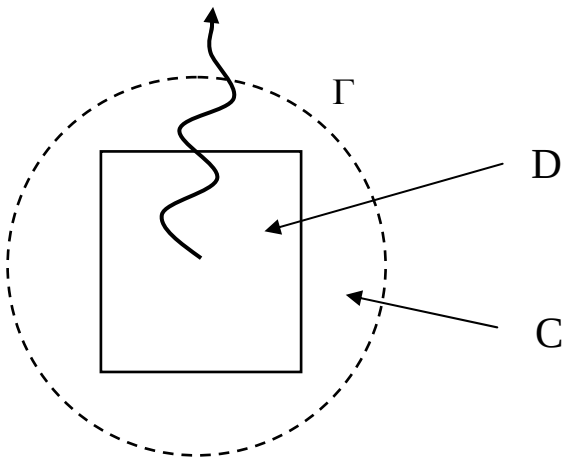

Figure 1. Domain of interest D, computational domain C, and open boundary Γ

The domain of interest D drawn with a square is a domain where we want to know the solution. The computational domain C includes also a transitional region where grid of D is continuously adapted to the circular boundary. Such mapping is useful because TBCs can be efficiently generated on simple boundaries like a circle or a sphere. Thus we compromise the increasing computational resources by introducing transitional layer with the decreasing of the efforts required for TBCs.

In order to obtain TBCs a decomposition of the original problem in the unbounded domain onto the interior and exterior problems is used; a non-local relationship on Γ is derived such that any solution to the exterior problem satisfies it (e.g. for the wave equation this is relationship between function and its first normal and time derivatives). Evidently the relationship uses the correspondent Green's function. Our approach of generating TBCs is based on spectral approximations of such Green's functions obtained analytically or numerically.

As an example consider TBCs on the circle for 2D wave equation in polar coordinates:

$$u_{tt} - \frac{1}{r}\left(r u_r\right)_r - \frac{1}{r^2} u_{\theta\theta} = 0 . \tag{1}$$

Denote by Q and Q^{-1} the direct an inverse Fourier operators for imaginary exponentials on Γ. The TBCs have the form, see Ref.[7] for details:

$$u_t + u_r + \frac{1}{2r} u = \frac{1}{2r^2} Q^{-1}\{B_k *\} Q u \tag{2}$$

where $\{B_k *\}$ are the time convolution operators for k-th Fourier harmonic with a kernel $B_k(t)$. Analytical formulas for $B_k(t)$ are known for this case but in practice we use the approximations by a sum of exponentials instead:

$$B_k(t) \approx \sum_{l=1}^{L_k} a_{l,k} \exp(b_{l,k} t), \quad \operatorname{Re} b_{l,k} \le 0 .$$

The benefits of such approximation are

1. Convolution with the sum of the exponentials is treated by recurrent formulas

$$\begin{aligned} A(t) := \int_0^t e^{b(t-t')} f(t')\,dt' &= \int_0^{t-\tau} e^{b(t-t')} f(t')\,dt' + \int_{t-\tau}^{t} e^{b(t-t')} f(t')\,dt' = \\ &= e^{b\tau} A(t-\tau) + \int_{t-\tau}^{t} e^{b(t-t')} f(t')\,dt' \end{aligned} , \tag{3}$$

   therefore one does not need to keep in memory the whole solution history on the boundary; it is enough to keep just one time layer for all number of exponentials L_k.

2. A relatively small number of exponentials L_k is enough to achieve a high accuracy of the approximation; the estimation $L_k \sim \log k$ for large k is proved in Ref.[10]. In practice the number of exponentials is less than 50 for most cases.

The recurrence treatment of convolution, firstly applied for nonreflecting boundary conditions problem in Ref.[6], drastically reduces the amount of work required.

Before pass to numerical examples let us make two remarks.

In a number of problems one needs an estimation of the far field solution. Transparent boundary conditions allow doing it correctly, since from the mathematical point of view the received solution in the computational domain can be reconstructed in the exterior according to the original governing equations. For calculation of the far field it is necessary to keep solution history on Γ and, for example, to take advantage of the formulas accompanying derivation of TBCs[6].

If an anisotropic media like layered, composite and others are considered, all abovementioned approaches of generating TBCs do not work. PML-based boundary conditions can also fail[15]. Recently we proposed *quasi-analytic* approach of calculating TBCs operator, Ref.[16] that can treat anisotropic and heterogeneous media.

3. TEST FROM THE SECOND COMPUTATIONAL AEROACOUSTICS WORKSHOP ON BENCHMARK PROBLEMS, SEE REF.[17]

We consider 2D wave equation (1) and the geometry shown in Figure 2. An obstacle O of circular shape with radius $r = 0.5$ is in the center of the computational domain C of radius $r = 5$ with boundary Γ. The initial conditions $u\big|_{t=0} = 2^{-25\left((x-4)^2+y^2\right)}$ and $u_t\big|_{t=0} = 0$ contain perturbations concentrated in the subdomain S. The impulse appeared due to the perturbations scatters by the obstacle and dissipates in the infinity.

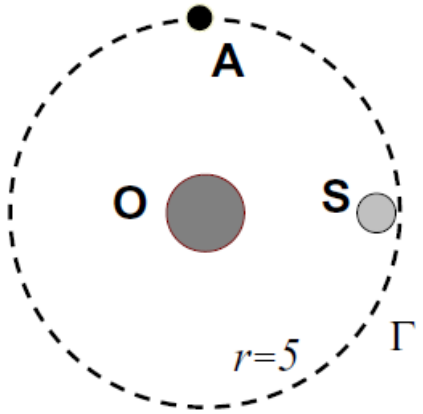

Figure 2. Computational domain C with the boundary Γ (dashed line), obstacle O, source domain S and observation point A

We use the equidistant 180×500 point polar grid in the half-space $y \ge 0$ due to the symmetry. The spatial steps are $h_r = 4.5/180$ and $h_\theta = \pi/500$, time step is $\tau = 0.0015$. Reference solution is calculated up to the time $t = 10$ on an extended domain of radius $r_{ext} = 10$.

TBCs (2) are used in our tests. To estimate the accuracy dependence versus the non-local part of TBCs we try several numbers of Fourier harmonics M in the numerical discretization of (2). The correspondent discrete formulas are denoted by $BCAT(M)$ and solutions by u_M. Also we consider the commonly used condition without non-local term in (2); it is denoted by $BC0$ (emphasize that it differs even from $BCAT(0)$ which treats only the zero harmonic). In Figure 3 the solutions $u_M(t)$ at point A with coordinates $r = 5$, $\theta = \pi/2$ are shown. Solution $BCAT(63)$ almost coincides with the reference solution. Also $BCAT(63)$ is more accurate than $BCAT(31)$ and $BC0$. In Figure 4 we draw L_2 – norms of the errors $\varepsilon_M(t)$ defined by

$$\varepsilon_M(t) = \left\| u_{ext}(t) - u_M(t) \right\|_{L_2(C \setminus O)}.$$

The solution for time $t = 7$, at $\theta = \pi/2$ and $0.5 \le r \le 5$ is shown in Figure 5. The difference between $BCAT(63)$ and reference solution is very small and can be hardly visible only at $r = 4.4$.

Also long time simulation up to time $t = 100$ has been done to verify the stability of calculations.

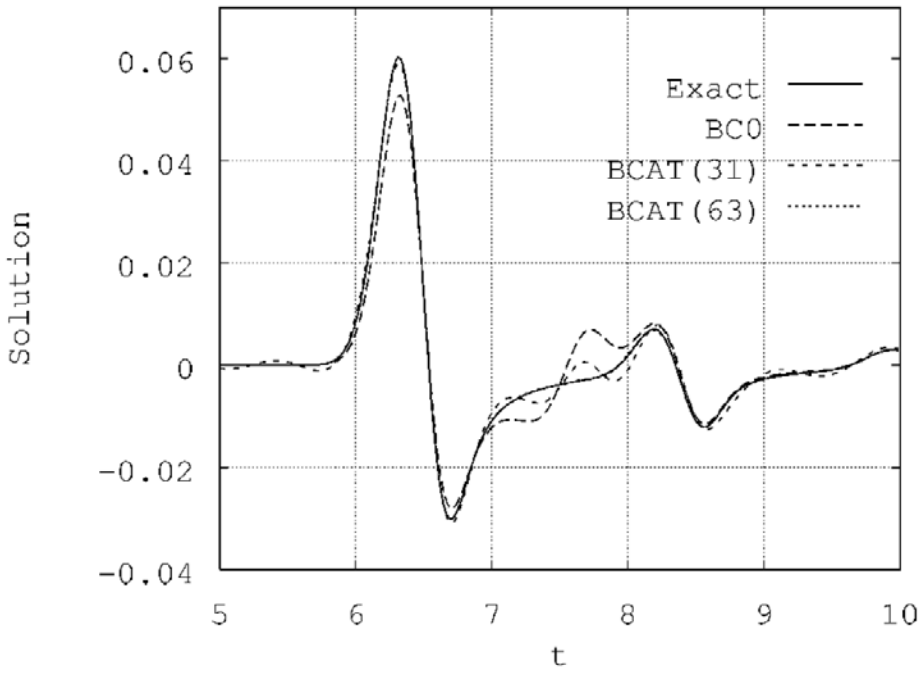

Figure 3. Solutions $BC0$, $BCAT(31)$, $BCAT(63)$ and reference solution versus time in spatial point $r = 5$, $\theta = \pi / 2$

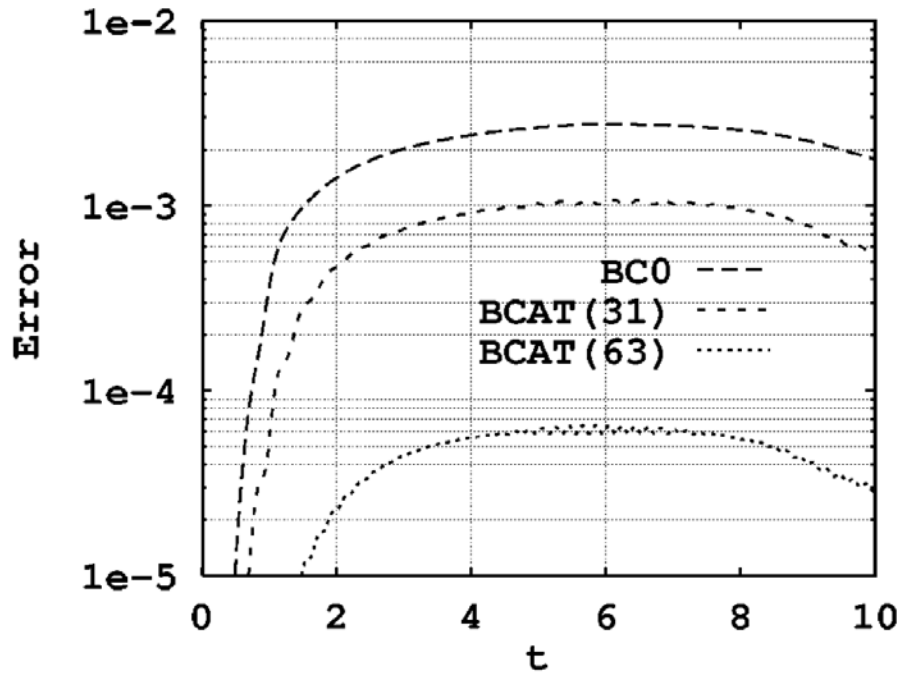

Figure 4. Errors $\varepsilon_0(t)$, $\varepsilon_{31}(t)$ and $\varepsilon_{61}(t)$

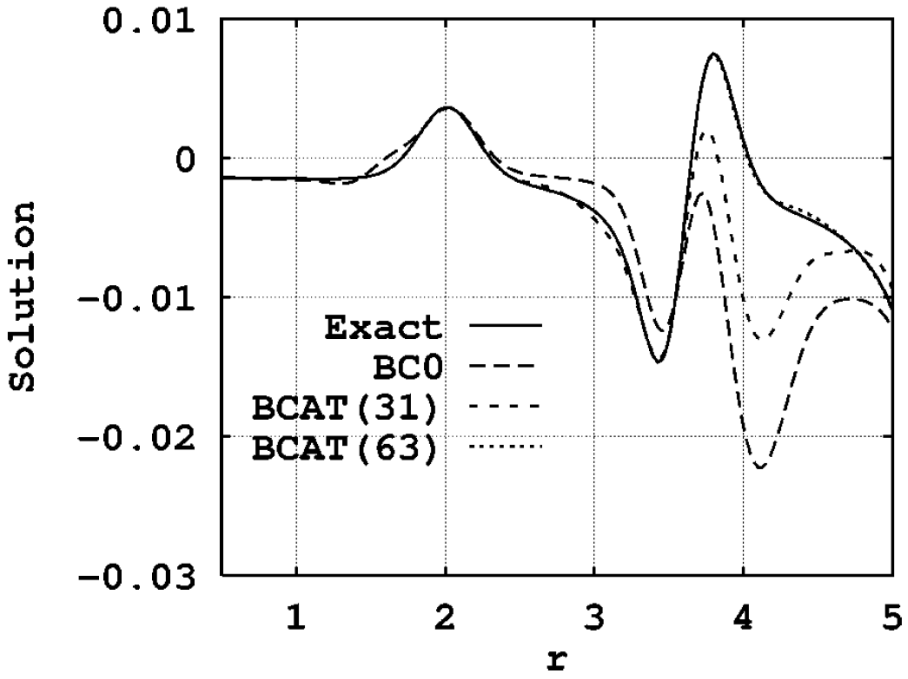

Figure 5. Solutions with $BC0$, $BCAT(31)$, $BCAT(63)$ and reference solution versus r at time $t = 7$ and azimuth $\theta = \pi / 2$

4. TBCs FOR EULER'S EQUATIONS AT INFLOW AND OUTFLOW OF A CHANNEL[8,18]

Application to the problem of a flow about the oscillating airfoil BAC 3-11/RES/30/21 in a channel is made in Ref.[18] where two types of the conditions are compared: TBCs and the commonly-used characteristics-based BCs.

Time-dependent flow problem about an airfoil in the infinitely long channel having the constant height outside a bounded computational domain is considered. The subsonic free-stream flow from $-\infty$ is constant, i.e. unsteadiness is caused strongly inside the computational domain (motion of the airfoil, flutter, separation etc). In order to find time-accurate transparent artificial boundary conditions at inlet and outlet cross-sections, we note that non-linear and viscous effects can be neglected far from the stream-lined body. Therefore we consider the time-dependent Euler equations linearised about the constant uniform background as a proper mathematical model in the far field. Analysis of this model permits to derive desired boundary conditions which are, naturally, non-local in both space and time. A special procedure to localize calculations with respect to time is used in order to sharply reduce computational costs without loss of accuracy[8,18].

4.1. Test problem and computational aspects

Unsteady flow about the oscillating airfoil BAC 3-11/RES/30/21 has been calculated for three different sizes of the channel: large (L), medium (M), and small (S), see Figure 6.

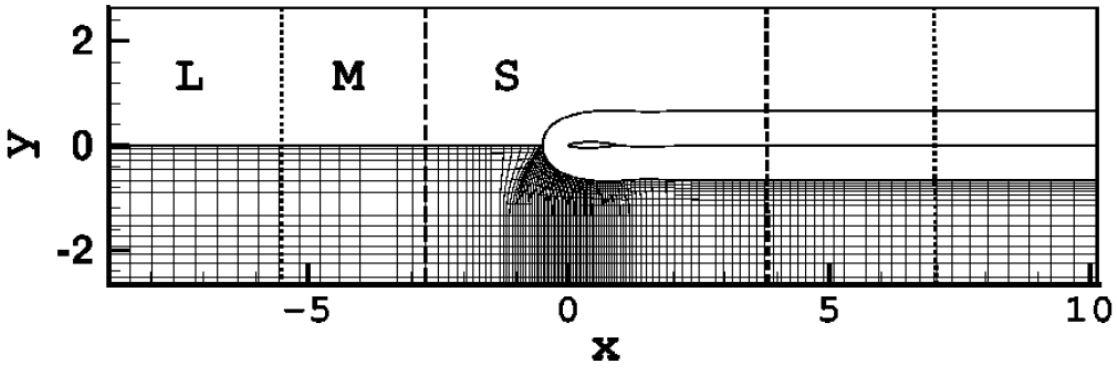

Figure 6. Geometry of three computational domains. Dotted and dashed lines denote the boundaries of the medium and small computational domains, respectively. The mesh in one of blocks is shown (thin lines are the internal boundaries of grid blocks)

The grid volume is 6912, 6144, 4864 cells for considered domains (grids for the smaller domains are subgrids of the large grid). Two types of boundary conditions are compared: TBCs and a certain kind of characteristic based boundary conditions implemented in the *FLOWer* code; we will denote the latter by CBCFs. The *FLOWer* code used for calculations, is being developed in the project MEGAFLOW by different German research organizations under leadership of DLR[19]. The algorithm is based on ideas of Ref.[20]. Central differences are used for the spatial discretization on structured grids. Time integration is performed by dual-time stepping. Grid generation is done using elliptical smoothing in every time step. Starting with a smoothed grid for the non-deformed reference configuration the grid is adapted algebraically to the current configuration. The nodes on the airfoil's surface are taken as material points throughout the motion, whereas the nodes at the outer boundary, which is the boundary of the computational domain, remain fixed in a rigid body fixed coordinate system. Thus, the grid is deforming with time and the nodes of the finite volumes within the flow field are moved such that a body surface fitting grid is ensured. Within each pseudo-time step an explicit multi stage Runge-Kutta method is used which is accelerated by techniques of local time stepping, enthalpy damping and implicit residual smoothing. The solution procedure is embedded into a sophisticated multigrid algorithm.

4.2. Results and conclusions

We prescribe the oscillations of the angle of attack of the airfoil by $\alpha(t) = \alpha_0 \sin(\omega t)$, $\alpha_0 = -3^o$. Figure 7 shows limit cycles of lift coefficient C_l versus time for the calculations with $M_\infty = 0.73$, reduced frequency $k = 0.28$ by using TBCs and CBCFs, respectively (the time is measured in seconds if the geometry sizes are in meters in Figure 6). The value $k = 0.28$ corresponds to so-called “resonance” case with maximal expected loss of accuracy of characteristic-based boundary conditions. We see that CBCFs give quite different solutions depending on the size of considered computational domains. On the other hand, TBCs provide convergence to a certain solution as the size of the computational domain increases (solid and dotted lines practically merge in the Figure 7, at the left). Therefore we can conclude about higher reliability of TBCs. Another observation obtained from numerous test calculations with CBCFs and TBCs is that the latter permits using much smaller sizes of the computational domain for computing both stationary and limit periodical solutions.

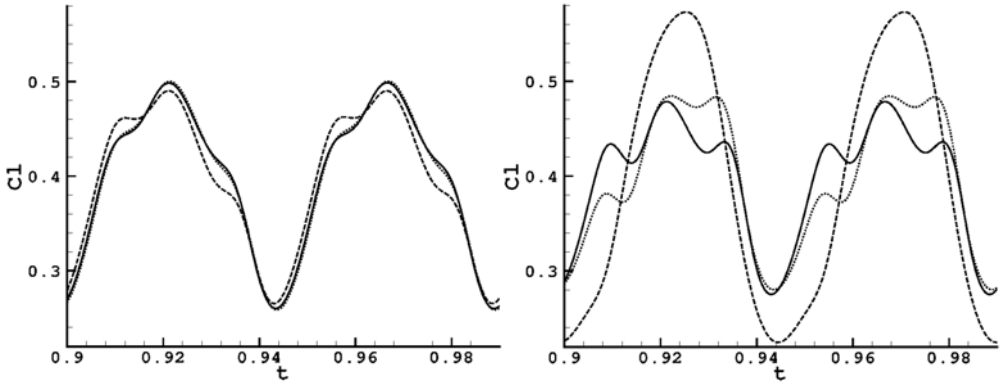

Figure 7. Graph $C_l(t)$ for the large (solid line), medium (dotted line), and small (dashed line) domains; $M_\infty = 0.73$, $k = 0.28$. Left: with TBCs; right: with CBCFs.

5. TBCs FOR MODEL PROBLEM IN MOVING MEDIA

We consider the problem of wave propagation in moving media described by the equation

$$u_{tt} + 2au_{tx} + a^2 u_{xx} - c^2(u_{xx} + u_{yy}) = 0 \tag{4}$$

where a is a given constant speed, c is the speed of sound, $0 \le a < c$. Transparent boundary conditions are generated on a circular boundary. Note that for $a = 0$ the desired TBCs are described in Section 2. An immediate treatment of (4) with $a > 0$ by the similar approach is not possible because of variable coefficients with respect to the azimuth angle: the Fourier method does not work. Here we use the method[21] for an approximate solution to this challenge. Idea consists of considering discrete counterparts of the original problems from the beginning with successive derivation and efficient approximation of correspondent discrete transparent boundary conditions (DTBCs).

We consider (4) in polar coordinates $x = r\cos\theta$, $y = r\sin\theta$ and apply a second order central-difference explicit scheme for the discrete function $u_{i,l}^p$ with indexes i in $r-$direction, l in azimuth direction, and p in time. Let index $i = I$ correspond to the open circular boundary Γ. Denote by $\left\{\varphi^m(\theta_l) = e^{im\theta_l}, m = 0,1,\ldots,M\right\}$ the discrete basis on the circular boundary. DTBCs permitting to calculate solution on Γ at time level $p+1$ from the updated solution in the internal points with $i = I-1$ have the form:

$$u_{I,l}^{p+1} = \sum_{m=0}^{M-1}\left\{\sum_{k=-m}^{M-1-m}\left(\mathcal{E}^{m,k}\right)^{p+1} * \hat{u}_{I-1,m}\varphi_l^{k+m}\right\} \tag{5}$$

where $\left(\mathcal{E}^{m,k}\right)^{p+1}$ are the coefficients of the DTBCs matrix; $\hat{u}_{I-1,m}$ denotes the Fourier coefficients of the solution at $i = I-1$; operation "*" denotes the discrete convolution with respect to time levels.

The DTBCs matrix is calculated in advance. Discrete convolution is treated by rapid recurrence formulas; therefore the extra computational costs of non-local operator (5) are of the same order as for the difference scheme in the interior.

5.1. Test calculations

In order to avoid singularities at the origin, the annular domain $1 \le r \le 2$ is considered. We impose homogeneous Dirichlet boundary conditions at $r = 1$ and our discrete non-local boundary conditions (5) at $r = 2$. The velocity $a = 0.2$ and $c = 1$.

Two equidistant meshes are used: coarse one with $h_r = 0.05$, $h_\theta = 2\pi/64$, $h_t = 0.03$, and fine one with $h_r = 0.025$, $h_\theta = 2\pi/128$, $h_t = 0.015$. Initial data is zero; the source $f(r,\theta,t) = q(t)g(|r - r_s|)p(\theta)$ is introduced by a right-hand side in the equation (4). Here $q(t)$ is the so-called Ricker signal with the central frequency $f_0 = 2$,

$$q(t) = \left(2\pi(f_0 t - 1)^2 - 1\right)e^{-\pi^2(f_0 t-1)^2}; \qquad g(r) = \begin{cases} e^{-r^2/(d^2-r^2)}, & |r| < d,\ d = 0.4 \\ 0, \text{ otherwise} \end{cases};$$

$$p(\theta) = \sin\theta + \sin 2\theta + \sin 3\theta + \sin 5\theta + \sin 7\theta.$$

Denote by S_E solutions calculated on the extended domain $1 \le r \le 10$ (to avoid spurious reflections at $1 \le r \le 2$ for $t < 15$), and also the reference solution $S_{E,R}$ obtained on the extended area with very fine mesh ($h_r = 0.00625$, $h_\theta = 2\pi/512$, $h_t = 0.00375$).

In Figure 8 at the left we represent the relative errors for $S_E - S_{E,R}$, i.e. the errors of the difference scheme approximation on our grids (all errors are measured in C-norm over the annular domain $1 \le r \le 2$. Note that the errors in L_2-norm have similar orders and behavior).

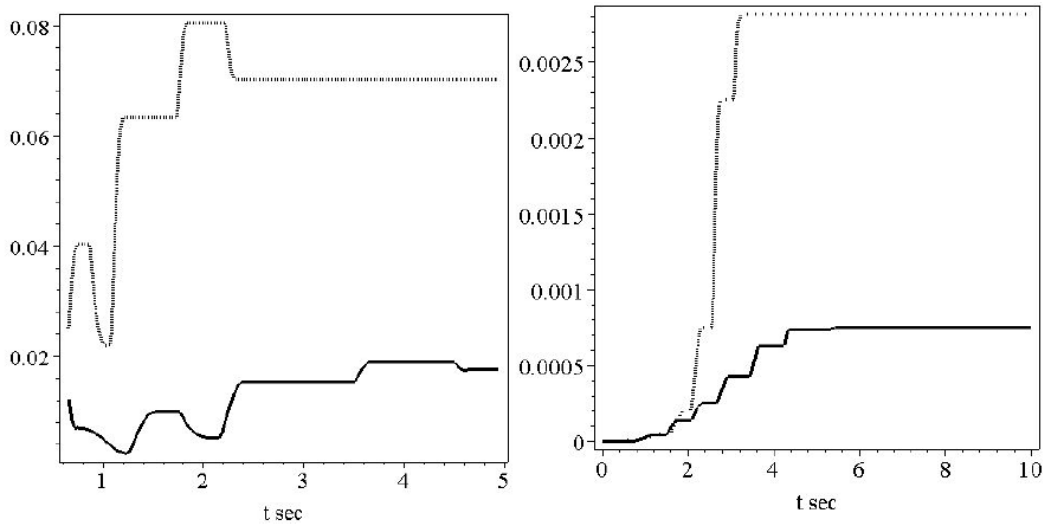

Figure 8. Errors of the solution calculated on extended domain. Left: $|S_{E,R} - S_E|_C / |S_E|_C$; right: $|S_E - S_{TBC}|_C / |S_E|_C$. Dashed line: coarse mesh $h_\theta = 2\pi/64$; solid line: fine mesh $h_\theta = 2\pi/128$

In Figure 8 at the right we represent the relative error for $S_E - S_{TBC}$ where S_{TBC} is obtained with DTBCs (5) at $r = 2$. Comparison of the left and right plots shows that errors due to reflections from open boundary are much less than the difference scheme

approximation errors (20 to 30 times), i.e. the error $\left|S_{E,R} - S_{TBC}\right|_C / \left|S_{E,R}\right|_C$ will have the same plot as in Figure 8 at the left.

Note that if we use a local boundary condition at $r = 2$ like $BC0$ mentioned in Section 3 then the errors have the values comparable to the solution, i.e. relative errors are about 1.

6. TBCs ON THE SIDE BOUNDARY FOR WAVE PROBLEMS IN CYLINDRICAL COMPUTATIONAL DOMAINS

We consider the wave equation

$$-\frac{1}{c^2}v_{tt} + v_{zz} + \frac{1}{r}(rv_r)_r = 0$$

in cylindrical coordinates (z,r); c is a constant speed of waves propagation. Denote by Γ_s the side boundary of a cylindrical domain D with radius R. Initial data are located inside D. Corresponding TBCs on Γ_s are proposed in Ref.[22]. They use Green's functions calculated for separate $z-$harmonics. For simplicity we suppose that domain D is closed by cross-sections $z = -Z$ and $z = Z$ where uniform Dirichlet boundary conditions are put. Actually $|Z|$ is large enough so that reflections from cross-sections come back to domain of interest after a prescribed simulation time.

We expand u in the Fourier series with respect to z

$$u(t,z,r) = \sum_{k=1}^{\infty} u^k(t,r)\sin\frac{k\pi}{Z}z$$

and denote by Q and Q^{-1} correspondent operators of the Fourier expansion. For each harmonic $u^k(t,r)$ at $r = R$ TBCs have the form:

$$T^k u^k := \frac{1}{c}\frac{\partial u^k}{\partial t} + \frac{\partial u^k}{\partial r} + \frac{1}{2R}u^k - \int_0^t B^k(t-t',R)u^k(t',R)dt' = 0 \qquad (6)$$

where $B^k(t,R)$ is the inverse Laplace transform of the function

$$\sqrt{(s/c)^2 + \lambda_k^2}\,\frac{K'_0(R\sqrt{(s/c)^2 + \lambda_k^2})}{K_0(R\sqrt{(s/c)^2 + \lambda_k^2})} + \frac{s}{c} + \frac{1}{2R}, \quad \lambda_k = \frac{k\pi}{Z},$$

$K_0(x)$ is the modified Bessel function of zero order.

Transparent boundary conditions on condition Γ_s are:

$$Q^{-1}\{T^k\}Qu = 0. \qquad (7)$$

For efficient treatment of (6) we approximate $B^k(t,R)$ by sums of exponentials:

$$\tilde{B}^k(t,r) := \sum_{m=1}^{M} \alpha_m e^{\beta_m t} \approx B^k(t,r), \quad \mathrm{Re}(\beta_m) < 0.$$

This approximation uses an array of numbers that has been calculated in advance ones and for all.

6.1. Example of test calculations.

We take the following geometry and mesh parameters for a test problem. Domain of interest D is $-1.5 \le z \le 1.5$ and $0 \le r \le R$, $R = 0.05$. Computational domain is extended in $z-$direction up to $-8 \le z \le 8$. Mesh has steps $h_z = 3/1536$, $h_r = 0.05/32$, $\tau = 3.125 \times 10^{-7}$. Speed of sound $c = 3000$; the boundary condition (7) is imposed at $r = R$. The source of initial impulse is located near the bottom of D. The impulse with respect to time has the form of the first derivative of the Black-Harris function $f(t) = 0.35322222 - 0.488\cos(2\pi t) + 0.145\cos(4\pi t) - 0.01022222\cos(6\pi t)$ with the central frequency about 10kHz. The simulation time $T = 0.004$.

Figure 9 shows the calculated solution with respect to time in the point near the top of D, the arrival time of impulse is about 0.001; the close-up with 100 times smaller scale of the amplitude is shown in Figure 10. Parameters of discretization of (7) are chosen so that the maximal amplitude of the reflection noise is less than 0.3% compared with the magnitude of impulse; this accuracy matches the accuracy of difference scheme for the wave equation in this test. Note that wall clock time to treat boundary conditions was 60% of total time.

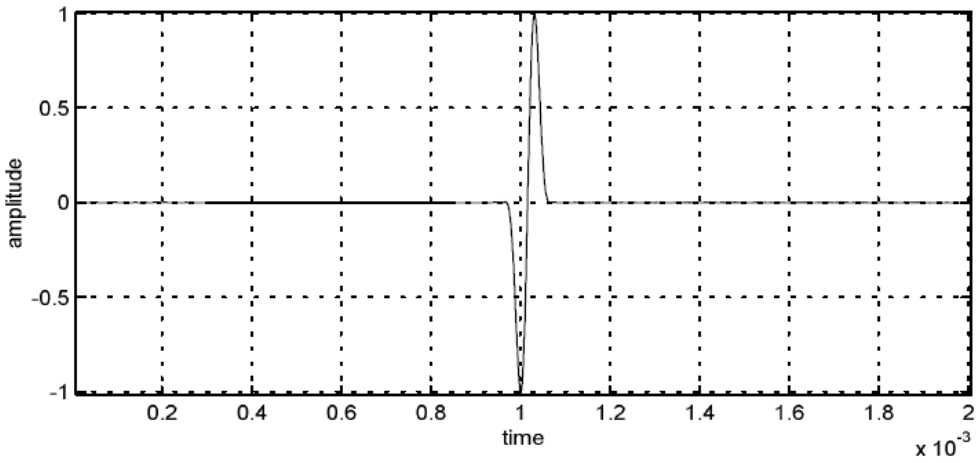

Figure 9. Amplitude of the solution versus time

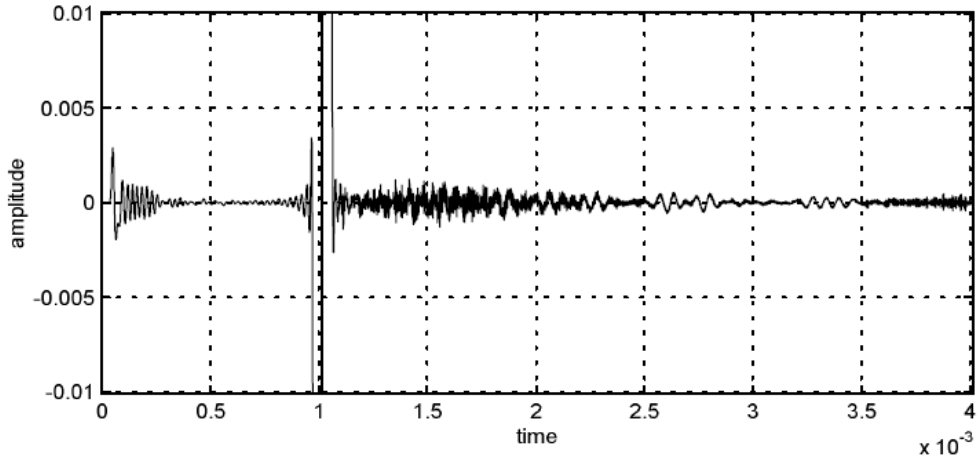

Figure 10. Close-up of the previous graph

7. REFERENCES

[1] A.S. Lyrintzis, "Review: The Use of Kirchhoff's method in computational aeroacoustics", *Journal of Fluids Engineering*, V. 116, No. 12, 665–676 (1994).

[2] S.V. Tsynkov, "Numerical solution of problems on unbounded domains", *Appl. Numer. Math.*, V. 27, P. 465–532 (1998)

[3] T. Hagstrom, "New results on absorbing layers and radiation boundary conditions", *Topics in Computational Wave Propagation*, M. Ainsworth, P. Davies, D. Duncan, P. Martin, and B. Rynne, eds., Springer-Verlag, P. 1-42 (2003)

[4] D. Givoli, "High-Order Local Non-Reflecting Boundary Conditions: A Review", *Wave Motion*, Vol. 39, P. 319-326 (2004)

[5] V.S. Ryaben'kii, *Method of Difference Potentials and Its Applications*, Fizmatlit, Moscow, 2002; Springer-Verlag, Berlin (2002)

[6] I.L. Sofronov, "Conditions for complete transparency on a sphere for the three-dimensional wave equation", *Russ. Acad. Sci. Dokl. Math.* 46, No. 2, 397-401 (1993).

[7] I.L. Sofronov, "Artificial boundary conditions of absolute transparency for two- and three-dimensional external time-dependent scattering problems", *Euro. J. Appl. Math.*, V. 9, No.6 , 561—588 (1998).

[8] I.L. Sofronov, "Non-reflecting inflow and outflow in wind tunnel for transonic time-accurate simulation", *J. Math. Anal. Appl.*, V. 221, 92–115 (1998).

[9] T. Hagstrom, "Radiation boundary conditions for the numerical simulation of waves", *Acta Numer.* Vol. 8, 47-106 (1999).

[10] B. Alpert, L. Greengard, and T. Hagstrom, "Nonreflecting Boundary Conditions for the Time-Dependent Wave Equation", *Journal of Computational Physics*, Vol. 180, 270-296 (2002).

[11] V.S. Ryaben'kii, V.I. Turchaninov, and S.V. Tsynkov, “On Lacunae-Based Algorithm for Numerical Solution of 3D Wave Equation for Arbitrarily Large Time”, *Mathematical Modeling,* 11, No. 12, pp. 113-127 (1999) [Russian]

[12] M. Grote, J. Keller, “Exact nonreflecting boundary conditions for the time dependent wave equation”, *SIAM J. Appl. Math.* , V. 55, No. 2 (1995).

[13] M. Grote, “Nonreflecting Boundary Condition for Elastodynamic Scattering”, *J. Comput. Phys.* Vol. 161, 331–353 (2000).

[14] J.P. Berenger, “A perfectly matched layer for the absorption of electromagnetic waves”, *Journal of Computational Physics,* Vol. 114 No. 2, p. 185-200, (1994)

[15] E. Becache, S. Fauqueux, P. Joly, “Stability of perfectly matched layers group velocities and anisotropic waves”, *JCP*, 188, 399–433 (2003).

[16] I. Sofronov, N. Zaitsev, “Transparent boundary conditions for the elastic waves in anisotropic media”, in *Proceedings of Eleventh International Conference on Hyperbolic Problems Theory, Numerics, Applications.* Ecole Normale Superieure de Lyon, Lyon, France, 17-21 July 2006. Accepted for publication.

[17] Second Computational Aeroacoustics Workshop on Benchmark Problems. Held 4-5 November 1996 in Florida State University, Tallahassee, Florida. Proceedings. NASA Conf. Publication 3352

[18] J. Ballmann, G. Britten, I. Sofronov, “Time-accurate inlet and outlet conditions for unsteady transonic channel flow”, *AIAA Journal,* Vol. 40, No. 2, 1745-1754 (2002).

[19] N. Kroll, R. Radespiel, C.C. Rossow, “Accurate and efficient flow solvers for 3D applications on structured meshes”, *Lecture Series 1994-05 of the von Karman Institute of Fluid Dynamics,* (1994).

[20] A.J. Jameson, “Time dependent calculation using multigrid, with applications to unsteady flows past airfoils and wings”, *AIAA-Paper 91-1596* (1991)

[21] I.L. Sofronov, O.V. Podgornova, “A spectral approach for generating non-local boundary conditions for external wave problems in anisotropic media”, *Journal of Scientific Computing,* V. 27, No 3, pp. 419-430 (2006).

[22] I.L. Sofronov, N.A. Zaitsev, “Transparent artificial boundary conditions for waves leaving a highly-stretched cylindrical computational domain”. *Preprint No. 80, Keldysh Inst. Appl. Math. Rus. Ac. Sci.* (1999)